Available online at www.sciencedirect.com
SCIENCE DIRECT®
ELSEVIER
International Journal of Solids and Structures 43 (2006) 3960–3982
INTERNATIONAL JOURNAL OF SOLIDS and STRUCTURES
www.elsevier.com/locate/ijsolstr

A solution of steady-state fluid flow in multiply fractured isotropic porous media

Pantelis A. Liolios, George E. Exadaktylos *

Mining Engineering Design Laboratory, Department of Mineral Resources Engineering, Technical University of Crete, University Campus, GR-73100 Chania, Greece

Received 4 March 2005
Available online 22 April 2005

Abstract

Herein a plane, steady-state fluid flow solution for fractured porous media is first presented. The solution is based on the theory of complex potentials, the theory of Cauchy integrals, and of singular integral equations. Subsequently, a numerical method is illustrated that may be used for the accurate estimation of the pore pressure and pore pressure gradient fields due to specified hydraulic pressure or pore pressure gradient acting on the lips of one or multiple non-intersecting curvilinear cracks in a homogeneous and isotropic porous medium. It is shown that the numerical integration algorithm of the singular integral equations is fast and converges rapidly. After the successful validation of the numerical scheme several cases of multiple curvilinear cracks are illustrated.

Keywords: Fault; Crack; Pore pressure; Fluid gradient; Complex potentials; Cauchy integrals; Singular integral equations

1. Introduction

There is a class of porous media problems for which the assumption of a single continuous porosity is not realistic. For example we refer here to the case of rock masses that are transected by pre-existing discontinuities such as faults, joints or cracks. These media which exhibit a "local preference" for fluid flow are called double porosity media or media with two (or more) degrees of porosity (Barenblatt et al., 1960; Warren and Root, 1963, among others).

* Corresponding author. Tel.: +30 28210 37690; fax: +30 28210 37891.
E-mail address: exadakty@mred.tuc.gr (G.E. Exadaktylos).

0020-7683/$ - see front matter © 2005 Elsevier Ltd. All rights reserved.
doi:10.1016/j.ijsolstr.2005.03.021

Pore fluids are believed to be involved in many dynamical processes related to seismic activity. These include the faulting process itself as well as postseismic phenomena caused by stress changes which result from seismic fault slip. Pore pressure build-up and release may play significant role in the seismic cycle and particularly in the initiation of faulting. Hickman et al. (1994) and Evans and Wong (1992) cite many papers which discuss the role of pore fluids in faulting processes. A better understanding of the fractured Earth's crust as a fluid-saturated poroelastic material is necessary in order to understand the physics of the entire earthquake cycle.

The study of fluid flow in fractured media has also many other significant practical applications such as:

- Hydraulic fracturing in boreholes in petroleum or geothermal reservoirs in order to increase the permeability of the formation.
- Pore pressure influence on fracture propagation in rocks and in situ stress measurements with the hydraulic fracturing technique.
- Estimation of the permeability of fluid reservoirs (e.g. petroleum, water).
- Hydro-mechanical erosion of rocks around wellbores.
- Rock fracturing with thermal fatique since the solutions of thermal and fluid flow problems are similar.

It is worth noticing here that in the first two classes of problems the pore pressure diffusion along the lips of the crack(s) is usually ignored.

For the study of problems of pore pressure or heat diffusion (potential flow theory) in fractured media, many different approaches can be used:

(1) Integral transform techniques such as Fourier, Mellin and Laplace transformations Sneddon (1951), among others, that can be applied in a small class of problems even though they may be significantly extended by the Wiener–Hopf technique (e.g. straight or semi-infinite cracks in the plane or in the half plane).
(2) Finite element (FEM) and finite difference (FDM) methods that are also called domain methods (Reddy, 1993, among many others) which have small accuracy along the crack boundaries.
(3) Boundary element methods (BEM) that require discretization only on the crack boundaries and boundaries of the domain and are accurate on the boundaries provided that special crack tip elements are employed (Brebbia and Dominguez, 1989; Banerjee and Butterfield, 1981; Brebbia et al., 1984; Hartmann, 1989, among many others).
(4) Complex potentials in conjunction with the theories of Cauchy integrals and of singular integral equations, which require more elaborate formulation but they lead to elegant closed-form or semi-analytical solutions (Mikhlin, 1957; Parton and Morozov, 1978; Barzokas and Exadaktylos, 1995). This method leads also to more accurate and time effective solutions compared to all the aforementioned numerical techniques (i.e. FEM, FDM, BEM).

The approach, which is followed here, is based on the latter method and on the Gauss–Chebyshev numerical integration scheme. The innovative character of the present solution lies in the fact that it can be applied for the general case of multiple non-intersecting curvilinear cracks where the shape of each crack may not be reduced to a known equation. Furthermore, it is demonstrated that the proposed solution converges rapidly to a stable estimation. Hence, it may be used to test the accuracy of a numerical code (such as FEM, FDM or BEM), as a tool for quick back analysis of in situ fluid flow or pore pressure measurements, and as a supplement to another numerical code for coupled thermo-hydro-mechanical problems.

2. Formulation of the equations for the fractured porous medium

2.1. General equations

By assuming that fluid flow is governed by Darcy's law, the permeability of the medium does not depend on the pore pressure and we have reached steady-state flow, then the mass balance leads to the well-known Laplace's equation for the pore pressure $p(x,y)$ in the plane Oxy of an isotropic porous medium, i.e.

$$\nabla^2 p(x,y) = \frac{\partial^2 p(x,y)}{\partial x^2} + \frac{\partial^2 p(x,y)}{\partial y^2} = 0 \tag{1}$$

In this work we assume that all the points on the plane Oxy correspond to the same geodetic height that is located below the phreatic surface (fully saturated medium). The solution of this field equation may be put in the following complex form:

$$\frac{\partial}{\partial z}\left(\frac{\partial}{\partial \overline{z}} p(z)\right) = 0 \tag{2}$$

The general solution of (2) is the following:

$$p(z) = \Phi(z) + \overline{\Phi(z)} = 2\mathrm{Re}(\Phi(z)) \tag{3}$$

where $\Phi(z)$ is an analytic function of the complex variable z with $z = x + \mathrm{i}y$, $\mathrm{i} = \sqrt{-1}$ is the imaginary unit, $\mathrm{Re}(\cdot)$ denotes the real part of what it encloses and the overbar denotes complex conjugate. Further, the fluid mass flow or specific discharge vector $q[L/T]$ is given by Darcy's law as follows:[1]

$$q(z) = -\lambda \,\mathrm{grad}\, p(z) = -\lambda\left(\frac{\partial p(z)}{\partial x} + \mathrm{i}\frac{\partial p(z)}{\partial y}\right) \tag{4}$$

where λ denotes the permeability coefficient $[L^4/(T \cdot F)]$ of the porous medium.

The boundary conditions of fluid flow encountered in practice are:

(1) Boundary conditions of the first kind, or Dirichlet b.c.'s, when the values of pore pressure are given at all points of the surface of the body

$$p = f_1(x,y) \tag{5}$$

(2) Boundary conditions of the second kind, or Neumann b.c.'s, when the values of the normal or tangential component of fluid discharge vector are given at all points of the surface of the body

$$\lambda \mathrm{Re}(\mathrm{grad}\, p) = f_2(x,y) \tag{6}$$

or

$$\lambda \mathrm{Im}(\mathrm{grad}\, p) = f_2'(x,y) \tag{7}$$

The method which is applied to the solution of the problem, consists in the formulation of a system of singular integral equations similar to the method employed in the paper by Barzokas and Exadaktylos, 1995, albeit in a more simplified form. As it is illustrated in Fig. 1, an infinite isotropic plate S containing k_1 internal curvilinear cracks L_i $(i = \overline{1,k_1})$, M thin strip inclusions l_i $(i = \overline{1,M})$, N holes γ_i $(i = \overline{1,N})$, k_2 point pressure sources (or sinks) of powers q_i concentrated at the points b_i $(i = \overline{1,k_2})$ and is under the influence of a homogeneous fluid flow q_∞, is considered.

[1] The fluid equations and boundary conditions are expressed here in terms of pressure rather than hydraulic head.

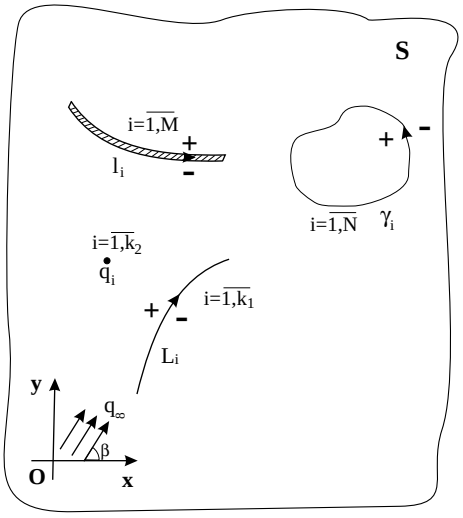

Fig. 1. Infinite isotropic medium containing k_1 curvilinear cracks, M thin inclusions, N holes and k_2 point sources (or sinks) subjected to a homogeneous fluid flow q_∞.

Depending on the nature of fluid flow conditions along the boundaries l_i, L_i and γ_i, we formulate the following boundary conditions:

$$p_*^{\pm}(t_0) = f_i^{\pm}(t_0) - p_0, \quad i = \overline{1, n_1} \tag{8}$$

$$-\lambda\left(\frac{\partial p_*}{\partial t_0}\right)^{\pm} = Q_i^{\pm}(t_0) - \lambda\frac{\partial p_0}{\partial t_0}, \quad i = \overline{n_1+1, k_1+M+N} \tag{9}$$

wherein t_0 is the complex coordinate of a point on the contours γ_i, l_i or L_i, n_1 is the number of boundaries on which Dirichlet boundary conditions are applied, Q_i is fluid flow vector in complex form and p_0 is the pressure induced by the point sources (or sinks) and the homogeneous fluid flow q_∞. Also, the plus of minus signs appearing as superscripts denote the limiting values of the respective functions as the boundary is approached from '+' or '−' side, respectively.

The pressure potential $\Phi(z)$ [$p(x,y) = 2\mathrm{Re}\Phi(z)$] of the steady-state fluid flow field $p(x,y)$ may then be expressed as follows:

$$\Phi(z) = \frac{q_\infty}{2} z\mathrm{e}^{-\mathrm{i}\beta} - \sum_{i=1}^{k_2}\frac{q_i}{2\pi\lambda}\ln(z-b_i) + \Phi_*(z) \tag{10}$$

where β is the angle of the homogeneous fluid flow q_∞ with the Ox axis and $\Phi^*(z)$ is given as

$$\Phi_*(z) = \frac{1}{2\pi}\left(\sum_{i=1}^{k_1}\int_{Li}\frac{\phi_{1i}\,\mathrm{d}t}{t-z} + \sum_{i=1}^{M}\int_{l_i}\frac{\phi_{2i}\,\mathrm{d}t}{t-z} + \sum_{i=1}^{N}\int_{\gamma_i}\frac{\phi_{3i}\,\mathrm{d}t}{t-z}\right) \tag{11}$$

with ϕ_{1i}, ϕ_{2i}, ϕ_{3i} being the real densities along the cracks, thin strip inclusions and holes, respectively.

Substituting in (8) and (9) the limiting values of the fluid flow potential given by (10), the following system of integral equations is obtained:

$$\frac{2}{\pi}\mathrm{Re}\left\{\int_{L^*_{mc}}\frac{\phi_{mc}(t)\,\mathrm{d}t}{t-t_0}+\sum_{\substack{i=1\\ i\neq c \text{ if } m=1}}^{k_1}\int_{L_i}\frac{\phi_{1i}(t)\,\mathrm{d}t}{t-t_0}+\sum_{\substack{i=1\\ i\neq c \text{ if } m=2}}^{M}\int_{l_i}\frac{\phi_{2i}(t)\,\mathrm{d}t}{t-t_0}+\sum_{\substack{i=1\\ i\neq c \text{ if } m=3}}^{N}\int_{\gamma_i}\frac{\phi_{3i}(t)\,\mathrm{d}t}{t-t_0}\right\}$$
$$=f_{2c}(t_0)-\mathrm{Re}\left(q_\infty t_0\mathrm{e}^{\mathrm{i}\beta}+\sum_{i=1}^{k_2}\frac{q_i}{\pi\lambda}\ln(t_0-b_i)\right)\quad t_0\in L_c,l_c,\gamma_c\quad c=\overline{1,n_1}\quad m=1,2,\text{ or }3 \tag{12}$$

where

$$f_{2c}(t_0)=f_c^+(t_0)+f_c^-(t_0) \tag{13}$$

and $L^*_{1c}=L_c,\ L^*_{2c}=l_c,\ L^*_{3c}=\gamma_c$.

$$\frac{2\lambda}{\pi}\mathrm{Re}\left\{\int_{L^*_{mc}}\frac{\phi_{mc}(t)\,\mathrm{d}t}{(t-t_0)^2}+\sum_{\substack{i=1\\ i\neq c \text{ if } m=1}}^{k_1}\int_{L_i}\frac{\phi_{1i}(t)\,\mathrm{d}t}{(t-t_0)^2}+\sum_{\substack{i=1\\ i\neq c \text{ if } m=2}}^{M}\int_{l_i}\frac{\phi_{2i}(t)\,\mathrm{d}t}{(t-t_0)^2}+\sum_{\substack{i=1\\ i\neq c \text{ if } m=3}}^{N}\int_{\gamma_i}\frac{\phi_{3i}(t)\,\mathrm{d}t}{(t-t_0)^2}\right\}$$
$$=Q_{2c}(t_0)+\lambda\mathrm{Re}\left(q_\infty\mathrm{e}^{\mathrm{i}\beta}+\sum_{i=1}^{k_2}\frac{q_i}{\pi\lambda}\frac{1}{t_0-b_i}\right)\quad t_0\in L_c,l_c,\gamma_c\quad c=\overline{n_1+1,k_1+M+N}$$
$$m=1,2,\text{ or }3 \tag{14}$$

where

$$Q_{2c}(t_0)=Q_c^+(t_0)+Q_c^-(t_0) \tag{15}$$

It should be noted that the above Cauchy integrals referring to the thin strip inclusions do not possess poles at the tips in contrast to those referring to the cracks.

In this first attempt to solve the above problem we are concerned in the next paragraphs only with cracks, thus discarding the presence of thin inclusions and holes. Also, for brevity of presentation we discard uniform fluid flow at infinity and the influence of point sources.

2.2. Solution for a single crack

A single crack lying on the horizontal plane Oxy is first considered. Let us, also, suppose that the crack is subjected to either a known pore pressure or to a known fluid flow.

The unknown complex potential function $\Phi(z)$ of the steady-state pore pressure field can be expressed by a Cauchy integral along the boundary of the crack L as follows:

$$\Phi(z)=\frac{1}{2\pi}\int_L\frac{\phi(t)\,\mathrm{d}t}{t-z} \tag{16}$$

where $t\in L$ and $\phi(t)$ is the unknown density which is considered to be a real function. It is clear from (16) that the function $\Phi(z)$ is holomorphic in the entire region excluding L and that for large $|z|$

$$\Phi(z)=\mathrm{O}\left(\frac{1}{|z|}\right) \tag{17}$$

(since the crack has a finite length). By assuming that z does not lie on L we can write (16) in the form

$$\Phi(z)=U(x,y)+\mathrm{i}V(x,y)=\frac{1}{2\pi}\int_L\frac{\phi(t)\,\mathrm{d}t}{t-z} \tag{18}$$

Moreover, if we take under consideration that

$$t - z = re^{i\theta} \tag{19}$$

where $r = |t - z|$and $\theta = \theta(z,t) = \arg(t - z)$, then by taking logarithmic derivatives of (19) we get

$$\frac{dt}{t-z} = d\log r + id\theta \tag{20}$$

Substituting (20) in (18) and then separating the result into real and imaginary part we obtain

$$\Phi(z) = U(x,y) + iV(x,y) = \frac{1}{2\pi}\int_L \phi(t)\, d\log r + i\frac{1}{2\pi}\int_L \phi(t)\, d\theta \tag{21}$$

The real part $U(x,y)$ of $\Phi(z)$ represents a modified potential of a simple layer whereas the imaginary part $V(x,y)$ represents a potential of a double layer.

By combining Eqs. (21) and (3) we derive the equation for the calculation of the pore pressure

$$p(z) = 2\mathrm{Re}(\Phi(z)) = \frac{1}{\pi}\int_L \phi(t)\, d\log r = \frac{1}{\pi}\int_L \phi(t)\frac{dr}{r} \tag{22}$$

The physical meaning of Eq. (22) is that the pore pressure at every point z of the plane depends only on its inverse distance from every point t on L multiplied by the appropriate weight, which is represented by the density function $\phi(t)$ (Fig. 2).

By combining Eqs. (4) and (22) we end up with an equation that can be used for the calculation of the mass fluid flow in both x and y directions on any point z of the plane

$$q(z) = \frac{\lambda}{\pi}\int_L \phi(t)\frac{\cos\alpha}{r^2}\, dr + i\frac{\lambda}{\pi}\int_L \phi(t)\frac{\sin\alpha}{r^2}\, dr \tag{23}$$

where α is the angle subtended by the vector $\vec{tz}$ and the positive direction of the Ox axis.

2.3. Solution for multiple cracks

Since the solution for both boundary value problems referring to either prescribed pore pressure or fluid flow on a single crack has been derived, the next step is to extend it to a system of non-intersecting cracks.

Let us consider for this purpose that there are k_1 non-intersecting cracks. Then, on a point z on the plane Oxy that does not belong to L_i (where $i = 1,2,\ldots,k_1$) the pore pressure will be the result of the effect of all the cracks as follows:

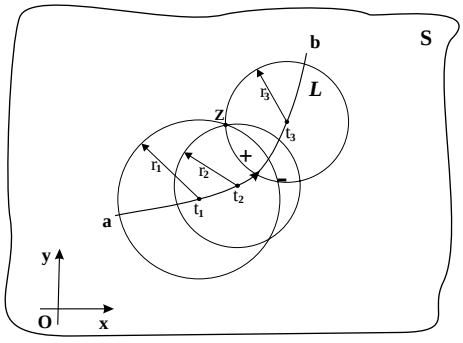

Fig. 2. Single internal curvilinear crack in an infinite plate. Contribution of each point t of L on the pore pressure to the point z of the plane.

$$p(z) = \sum_{i=1}^{k_1} \frac{1}{\pi} \int_{L_i} \phi_i(t) \frac{\mathrm{d}r}{r_i} \tag{24}$$

where $\phi_i(t)$, r_i are the density and the magnitude $|t - z|$of the ith crack respectively.

Working similarly as above, we derive the solution for the fluid flow

$$q(z) = \sum_{i=1}^{k_1} \frac{\lambda}{\pi} \int_{L_i} \phi_i(t) \frac{\cos \alpha_i}{r_i^2} \mathrm{d}r + \mathrm{i} \sum_{i=1}^{k_1} \frac{\lambda}{\pi} \int_{L_i} \phi_i(t) \frac{\sin \alpha_i}{r_i^2} \mathrm{d}r \tag{25}$$

where α_i is the angle between the vector $\vec{tz}$ of the ith crack and the positive direction of the Ox axis.

3. Numerical solution

In order to calculate the pore pressure and the fluid flow fields, one has to manage to define the unknown densities $\phi_i(t)$ such as to satisfy the boundary conditions along the cracks. This problem is well known as the inversion problem of the Cauchy integrals for arcs (Muskhelishvili, 1953). Although for simple cases it is possible to invert the Cauchy integral in closed form, in general it cannot be calculated easily. Herein we propose a numerical method that can be used for the calculation of the unknown densities and can be used even for the most complicated cases such as the system of non-intersecting curvilinear cracks of arbitrary shape. The proposed methodology will be presented in a hierarchical fashion beginning with the simplest cases and proceeding with more complicated ones.

3.1. Simple linear crack

3.1.1. Dirichlet boundary conditions

Let us consider a linear crack (Fig. 3). It is assumed that by some mechanism the pore pressure inside the crack attains a certain distribution instantly and this pore pressure remains constant through time. At sufficient large time for steady-state pore pressure diffusion to be reached, then according to (22) for a point t_0 that belongs to the crack L, the following equation holds true:

$$p(t_0) = \frac{1}{\pi} \int_L \phi(t) \frac{\mathrm{d}r}{|t - t_0|} \tag{26}$$

in which $p(t_0)$ denotes the Dirichlet boundary condition at point t_0 on L. The integral Eq. (26) is singular since for $t = t_0$ the quantity $1/|t - t_0|$is infinite. In order to calculate the unknown density $\phi(t)$ the Gauss–

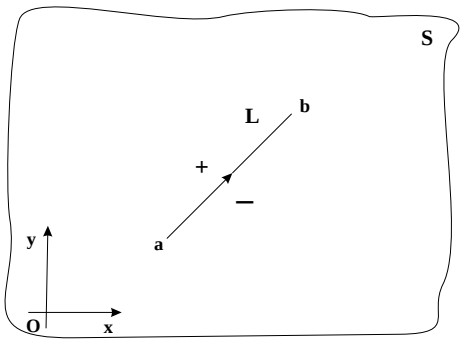

Fig. 3. A single straight crack and system of coordinates.

Chebyshev numerical integration method for singular integral equations will be employed (Erdogan and Gupta, 1972). This method displays high accuracy along the crack but it does not give estimates at the limits of the integration interval.

The endpoints a, b of the crack are points of geometric singularity. Physical arguments provide sufficient information about the behavior of the unknown density function $\phi(t)$. Invariably, these arguments simply account to stating that if the unknown function is a potential (i.e. temperature, pore pressure, displacement etc.) it has to be bounded at the singular points a, b. It can be shown that the fundamental function of (26) which characterizes the behavior of $\phi(t)$ at the singular points a and b is given by (Muskhelishvili, 1953; Erdogan, 1969):

$$w(t) = \sqrt{(t-a)(b-t)} \tag{27}$$

since $\phi(t)$ is bounded at these points. By applying numerical integration in (26) and taking under consideration (27) there results the following system of linear algebraic equations:

$$\frac{1}{\pi}\int_a^b \sqrt{(t-a)(b-t)}\,\frac{\hat{\phi}(t)}{|t-t_0|}\,\mathrm{d}t = p(t_0) \Longleftrightarrow \frac{1}{\pi}\sum_{j=1}^{n} w_j \frac{\hat{\phi}(t_j)}{|t_j - t_{0r}|} = p(t_{0r}) \tag{28}$$

where we have set $\phi(t) = w(t)\hat{\phi}(t)$, $\hat{\phi}(t)$ is the new unknown function that is bounded in the closed interval $[a,b]$ and satisfies the Hölder condition in order to ensure existence of the principal value of the Cauchy integral in (28), n is the number of integration points and r is the number of collocation points. The weight functions w_j are given by

$$w_j = \frac{\pi}{n+1}\sin^2\left(\frac{j\pi}{n+1}\right) \tag{29}$$

The integration points t_j and collocation points t_{0r} referring to the interval $[a,b]$ may be found by the linear transformation of the integration and collocation points ξ_j, η_r, respectively, referring to the interval $[-1,1]$ as follows:

$$t_j = \frac{b-a}{2}\xi_j + \frac{b+a}{2} \tag{30}$$

$$t_{0r} = \frac{b-a}{2}\eta_r + \frac{b+a}{2} \tag{31}$$

According to Erdogan and Gupta (1972) the integration points ξ_j are the roots of the Chebyshev polynomials of the second kind and of order n

$$\xi_j = \cos\left(\frac{j\pi}{n+1}\right), \quad j = 1,2,\ldots,n \tag{32}$$

while the collocation points η_r are the roots of the Chebyshev polynomials of the first kind and of order $(n+1)$

$$\eta_r = \cos\left(\frac{\pi(2r-1)}{2(n+1)}\right), \quad r = 1,2,\ldots,n+1 \tag{33}$$

Eq. (28) represents a linear system of $(n+1)$ algebraic equations with n unknowns, i.e. the densities $\hat{\phi}(t_j)$, $j = 1,2,\ldots,n$. Hence, the system is over-determined but in practice one can choose n to be an even integer

and ignore the equation that corresponds to $r = \frac{n}{2} + 1$ (Erdogan and Gupta, 1972). After the solution of (28), the pore pressure in the entire plane domain can be found as follows:

$$p(z) = \frac{1}{\pi} \sum_{j=1}^{n} w_j \frac{\hat{\phi}(t_j)}{|t_j - z|} \tag{34}$$

where z is an arbitrary point on the plane. The equation for the calculation of the fluid flow is derived for the Neumann boundary condition case that follows.

3.1.2. Neumann boundary conditions

Following a similar path, let us assume now that by some mechanism the fluid flow inside the crack attains a certain distribution instantly and this flow remains constant through time. In order to formulate the linear system of algebraic equations for the calculation of the unknown density, Eq. (23) is modified into a more convenient form. In fact, we will derive a similar form to (23) for a local coordinate system (s_0, n_0) that corresponds to a point t_0 that belongs to the crack, where s_0, n_0 are the tangent and the normal at t_0 respectively (Fig. 4). Then, by recalculating the gradient of the pore pressure (see (4)) in terms of the local coordinate system at t_0 we derive the modified form of (23)

$$q(t_0) = q_s(t_0) + \mathrm{i} q_n(t_0) = \frac{\lambda}{\pi} \int_L \phi(t) \frac{\cos \alpha(t, t_0)}{r^2} \, \mathrm{d}r + \mathrm{i} \frac{\lambda}{\pi} \int_L \phi(t) \frac{\sin \alpha(t, t_0)}{r^2} \, \mathrm{d}r \tag{35}$$

where $q_s(t_0)$, $q_n(t_0)$ are the tangential and the normal flow respectively and $\alpha(t, t_0)$ is the angle enclosed by the vector $t, \vec{t}_0$ and the positive tangent T_0 at the point t_0 (Fig. 4). The real part of Eq. (35) can be defined and calculated and it does not depend if point t_0 is approached from the upper (+) or the lower (−) side. However, the calculation of the imaginary part is altered if it is approached from the upper or the lower side (since the fluid flow that is perpendicular to the crack has opposite directions as we approach from the upper or the lower side). Hui and Mukherjee (1997) have proved that its value is not equal to zero and the density function can be calculated by virtue of an extended Plemelj formulae for hypersingular integrals. However, the latter gives the unknown density on t_0, hence interpolation is required in order to define the density on t for the full field domain solution. This means additional error due to numerical interpolation, as well as more complicated formulae.

As it is clear from (35), it suffices to prescribe only the one of the two flow vector components on the boundary in order to calculate the unknown density $\phi(t)$. Due to this fact and by taking under consideration the aforementioned analysis for the imaginary part of (35), we will employ here only the tangential fluid flow for the calculation of the unknown density.

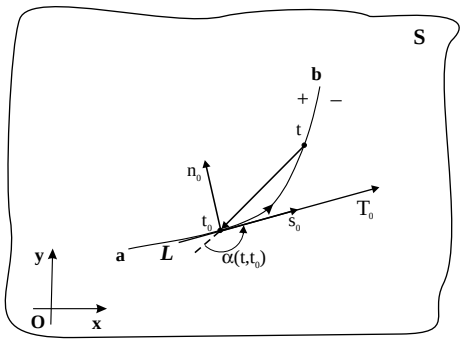

Fig. 4. Internal curvilinear crack in an infinite plate and local system of coordinates.

The tangential fluid flow $q_s(t_0)$ on a point t_0 of L is given by

$$q_s(t_0) = \frac{\lambda}{\pi} \int_L \phi(t) \frac{\cos \alpha(t, t_0)}{r^2} \, \mathrm{d}r \tag{36}$$

By applying to (36) the numerical integration scheme given by (28) we get

$$\frac{\lambda}{\pi} \sum_{j=1}^{n} w_j \frac{\hat{\phi}(t_j) \cos \alpha(t_j, t_{0r})}{|t_j - t_{0r}|^2} = q_s(t_{0r}) \tag{37}$$

where the weights w_j as well as the integration t_j and collocation t_{0r} points are calculated in a similar fashion to the Dirichlet case. In order the linear system of Eq. (37) to be soluble or at least the solution to produce flows that have physical meaning, one additional condition must be fulfilled. This condition is called the *Condition of Solubility* and prescribes that the integral of the tangential flow with respect to s_0 must be always null

$$\int_L q_s(t_0) \, \mathrm{d}s_0 = 0 \Rightarrow \sum_{r=1}^{n+1} q_s(t_{0r}) = 0 \tag{38}$$

This condition refers only to the profile of the tangential flow (Neumann b.c.) that is applied to the boundary and it is not part of the system of linear equations. However, it is necessary and suffice condition for the solubility of (38) (Muskhelishvili, 1953).

After the solution of (37), the fluid flow in both x and y directions at any point z of the plane can be calculated by applying a similar numerical integration to (23)

$$q(z) = q_x(z) + \mathrm{i} q_y(z) = \frac{\lambda}{\pi} \sum_{j=1}^{n} w_j \frac{\hat{\phi}(t_j) \cos \alpha(t_j, z)}{|t_j - z|^2} + \mathrm{i} \frac{\lambda}{\pi} \sum_{j=1}^{n} w_j \frac{\hat{\phi}(t_j) \sin \alpha(t_j, z)}{|t_j - z|^2} \tag{39}$$

Note that now α is the angle enclosed by the vector $\vec{tz}$ and the positive direction of the Ox axis.

3.2. Smooth curvilinear crack

The methods of numerical integration of Gauss–Chebyshev that were presented in the previous paragraph are not applicable for smooth curvilinear cracks of arbitrary shape. It shall be noted that in special cases where the crack L can be described by a known equation $z = z(s)$, where s is a real variable varying along L, then by modifying transformations (30) and (31) the problem may be easily reduced into a system of linear algebraic equations. However, in order to consider the general case of arbitrary crack shape, a methodology was developed here for the computation of the integration and the collocation points. This is based on the approximation of the crack by an adequate number of linear segments. The algorithm that is used for the computation of the coordinates of the integration and collocation points for both types of boundary conditions is the same, hence for the sake of brevity the methodology for the computation of coordinates of t_j is presented here. Also, it must be noted that this method can be used for higher order approximations of the crack shape (e.g. splines), but in order to preserve the simplicity of exposition of the theory we present here only the linear approximation.

The basic idea of the methodology has as follows: in a first step, the coordinates of the integration points ξ_j that correspond to the interval $[-1, 1]$ are transformed into a linear interval with a length equal to the total length of the curvilinear crack. At the same time the distances between the consecutive points on this new linear interval are calculated. Then, starting from the one crack tip (say tip a), the integration points are placed consecutively one-by-one along the curvilinar crack by measuring each time its known distance from the previous point.

Let us assume that K linear segments approximate a curvilinear crack (Fig. 5). All these linear segments have a total of $(K + 1)$ endpoints whereas the total length of the crack is the sum of their lengths

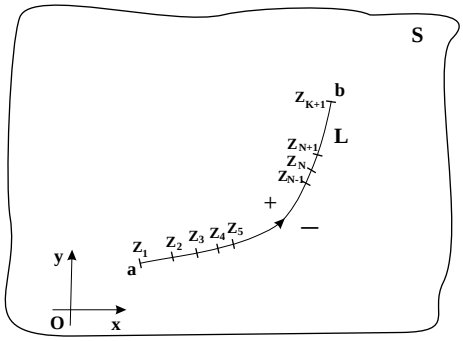

Fig. 5. Curvilinear crack discretized by K linear segments.

$$D = \sum_{N=1}^{K} \sqrt{(y_{N+1} - y_N)^2 + (x_{N+1} - x_N)^2} \tag{40}$$

in which D is the total length and x_N, y_N are the coordinates of the Nth endpoint.

Let us now set the origin of a new coordinate system to the one limit of the linear interval $[-1, 1]$, for example the right limit $(+1)$. One can compute the percentage of the total length of the linear interval $[-1, 1]$ in which every integration point $\xi_{j(\text{perc})}$ lies as follows:

$$\xi_{j(\text{perc})} = \frac{1 - \xi_j}{2}, \quad j = 1, 2, \ldots, n \tag{41}$$

where ξ_j are computed by virtue of Eq. (32). By setting the origin of another local coordinate system to the one tip of the curvilinear crack (for example the end a), it is possible to compute the distances (measuring from the tip a) on the crack L on which the points t_j must be placed, by multiplying the total distance D of the crack with the percentages $\xi_{j(\text{perc})}$

$$t_{j(\text{dist})} = \xi_{j(\text{perc})} D, \quad j = 1, 2, \ldots, n \tag{42}$$

Subsequently, the distance between two consecutive integration points can be calculated by the following equation:

$$\Delta t_j = \begin{cases} t_{1(\text{dist})} & \text{if } j = 1, \\ t_{j(\text{dist})} - t_{j-1(\text{dist})} & \text{if } j > 1, \end{cases} \quad j = 1, 2, \ldots, n \tag{43}$$

Also, the vector of the cumulative lengths of the linear segments, which approximate the curvilinear crack, has the following form:

$$D_{(\text{cum})} = \left[D_1, D_1 + D_2, \ldots, \sum_{N=1}^{K} D_N \right] \tag{44}$$

where D_N is the length of the Nth linear segment.

Since there are n points t_j the algorithm must be repeated n times. Also, a new variable, called *Distance Meter* (DM) that is a distance and is defined below, should be computed in each loop that will be used later for correcting the placement of each integration point along the crack. Its initial value is set equal to zero. Moreover, one has to set an initial base point which in this case will be the end a of the crack L (it must be the same with the origin of the local coordinate system which was used for Eq. (42)) with coordinates x_a, y_a. Finally, we define as $D_{N(\text{cum})}$ as the Nth entry in the vector of the cumulative lengths $D_{(\text{cum})}$ and we set the initial value of N equal to 1. The initial conditions have as follows:

$$\begin{aligned} \mathrm{DM} &= 0 \\ x_{\mathrm{base}} &= x_a \\ y_{\mathrm{base}} &= y_a \\ N &= 1 \end{aligned} \tag{45}$$

The algorithm has as follows:

If the sum of the DM with the current Δt_j is smaller than the current $D_{N(\mathrm{cum})}$, then the following steps are followed:

(1) The current t_j is calculated from the formula

$$t_j = \Delta t_j \mathrm{e}^{\mathrm{i}\omega} + (x_{\mathrm{base}} + \mathrm{i}y_{\mathrm{base}}) \tag{46}$$

in which ω is the angle subtended between the Ox axis and the current Nth linear segment of the curve measured in the positive direction (Fig. 6(a)).

(2) The new DM is the sum of the previous value of DM and the current value of Δt_j.

(3) The new base point is the current value of t_j.

Then, we return back to the start of the algorithm for the next loop. Fig. 6(a) illustrates graphically the procedure described for this case.

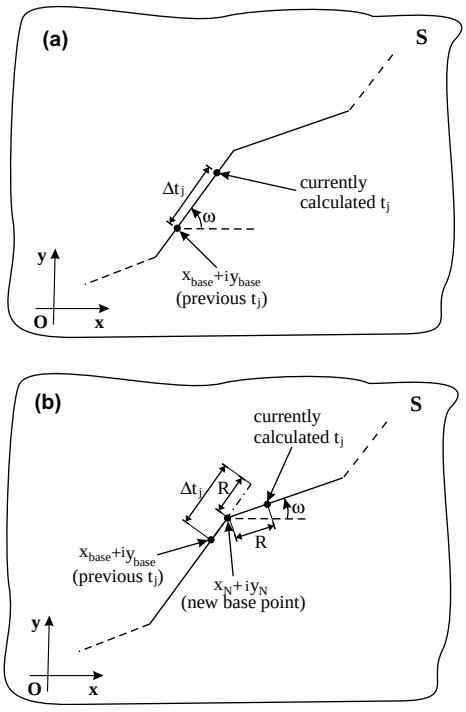

Fig. 6. Calculation of the integration points along a crack of arbitrary shape. (a) First case: The integration point that is currently calculated must be placed on the current linear segment. (b) Second case: The integration point that is currently calculated must be placed on the next linear segment.

On the other hand, if the sum of the DM with the current Δt_j is greater or equal to the current $D_{N(\mathrm{cum})}$ then the following steps are followed:

(1) A new variable which we call *Remaining* (R) is computed as follows:

$$R = \mathrm{DM} + \Delta t_j - D_{N(\mathrm{cum})} \tag{47}$$

(2) We increase the value of N by 1

$$N = N + 1 \tag{48}$$

(3) The new base point will be

$$\begin{aligned} x_{\mathrm{base}} &= x_N \\ y_{\mathrm{base}} &= y_N \end{aligned} \tag{49}$$

where x_N, y_N indicate the coordinates of the Nth endpoint of the linear segments of the curve L.

(4) If R is smaller than the length of the current length of the Nth linear segment of the curve then the current t_j is set equal to the following expression:

$$t_j = R\mathrm{e}^{\mathrm{i}\omega} + (x_{\mathrm{base}} + \mathrm{i}y_{\mathrm{base}}) \tag{50}$$

where ω is the angle between the Ox axis and the current linear segment of the curve (Fig. 6(b)).Else, if R is greater or equal to the current length of the Nth linear segment of the curve then a new R is calculated as follows:

$$R = R - \sqrt{(y_{N+1} - y_N)^2 + (x_{N+1} - x_N)^2} \tag{51}$$

and we go back again to step (48) of the 2nd case. This step ensures that we follow the curve in all possible cases.

(5) The new DM will be the sum of the old DM with the current Δt_j.

(6) The new base point is the current computed value of t_j.

Finally we return back to the start of the algorithm for the next loop. Fig. 6(b) illustrates graphically the procedure described for this case.

The above algorithm is executed for n loops until all the points t_j are computed. After all the integration and collocation points have been found, the pore pressure or the fluid flow can be computed in the manner that was presented in the previous paragraphs.

3.3. System of smooth non-intersecting curvilinear cracks

Let us assume a multiply fractured domain with k_1 non-intersecting cracks. Also, let us assume that the first n_1 cracks are under Dirichlet boundary conditions and the remaining $(k_1 - n_1)$ cracks are under Neumann boundary conditions.

By combining the integral Eqs. (24) and (26) we derive the integral equation for a point t_0 that belongs to a crack on which Dirichlet boundary condition is applied

$$p(t_{0c}) = \frac{1}{\pi}\int_{L_c} \frac{\phi_c(t)}{|t - t_{0c}|}\,\mathrm{d}r + \frac{1}{\pi}\sum_{\substack{i=1 \\ i\neq c}}^{k_1} \int_{L_i} \frac{\phi_i(t)}{|t - t_{0c}|}\,\mathrm{d}r, \quad c = 1, 2, \ldots, n_1 \tag{52}$$

where $p(t_{0c})$ is the Dirichlet boundary condition at the point t_0 of the cth crack. Eq. (52) in conjunction with (28) leads to the linear system of algebraic equations that refers to the Dirichlet boundary conditions

$$\frac{1}{\pi}\sum_{j=1}^{n} w_j \frac{\hat{\phi}_c(t_{jc})}{|t_{jc}-t_{0rc}|} + \frac{1}{\pi}\sum_{\substack{i=1\\ i\neq c}}^{k_1}\sum_{j=1}^{n} w_j \frac{\hat{\phi}_i(t_{ji})}{|t_{ji}-t_{0rc}|} = p(t_{0rc}), \quad c = 1,2,\ldots,n_1 \tag{53}$$

in which we have used for the sake of simplicity the same number of integration and collocation points for each crack. Eq. (53) consists a linear system of $(n_1 \times n)$ equations with $(k_1 \times n)$ unknowns. The remaining $((k_1 - n_1) \times n)$ equations that are necessary for the solution of the system will be derived by the Neumann boundary conditions.

By combining Eqs. (25) and (36) we derive the integral equation for a point t_0 that belongs to a crack on which Neumann boundary condition is applied

$$q_s(t_{0c}) = \frac{\lambda}{\pi}\int_{L_c} \frac{\phi_c(t)\cos\alpha(t,t_{0c})}{|t-t_{0c}|^2}\,\mathrm{d}r + \frac{\lambda}{\pi}\sum_{\substack{i=1\\ i\neq c}}^{k_1}\int_{L_i} \frac{\phi_i(t)\cos\alpha(t,t_{0c})}{|t-t_{0c}|^2}\,\mathrm{d}r, \quad c = n_1+1, n_1+2,\ldots,k_1 \tag{54}$$

where $q_s(t_{0c})$ is the tangential flow at the point t_0 of the cth crack. Eq. (54) in conjunction with (37) leads to the linear system of algebraic equations that refers to the Neumann boundary conditions

$$\frac{\lambda}{\pi}\sum_{j=1}^{n} w_j \frac{\hat{\phi}_c(t_{jc})\cos\alpha(t_{jc},t_{0rc})}{|t_{jc}-t_{0rc}|^2} + \frac{\lambda}{\pi}\sum_{\substack{i=1\\ i\neq c}}^{k_1}\sum_{j=1}^{n} w_j \frac{\hat{\phi}_i(t_{ji})\cos\alpha(t_{ji},t_{0rc})}{|t_{ji}-t_{0rc}|^2} = q_s(t_{0rc}), \quad c = n_1+1, n_1+2,\ldots,k_1 \tag{55}$$

Eqs. (53) and (55) consist a linear system of $(k_1 \times n)$ equations with $(k_1 \times n)$ unknowns (i.e. the unknown densities $\hat{\phi}_i(t)$).

After the computation of the crack densities the pore pressure and the fluid flow at any point z of the plane can be calculated by virtue of equations

$$p(z) = \frac{1}{\pi}\sum_{i=1}^{k_1}\sum_{j=1}^{n} w_j \frac{\hat{\phi}_i(t_{ji})}{|t_{ji}-z|} \tag{56}$$

and

$$q(z) = q_x(z) + \mathrm{i}q_y = \frac{\lambda}{\pi}\sum_{i=1}^{k_1}\sum_{j=1}^{n} w_j \frac{\hat{\phi}_i(t_{ji})\cos\alpha(t_{ji},z)}{|t_{ji}-z|^2} + \mathrm{i}\frac{\lambda}{\pi}\sum_{i=1}^{k_1}\sum_{j=1}^{n} w_j \frac{\hat{\phi}_i(t_{ji})\sin\alpha(t_{ji},z)}{|t_{ji}-z|^2} \tag{57}$$

respectively.

4. Numerical examples

Before proceeding to the presentation of numerical examples, it is necessary to check the convergence of the proposed numerical solution. Since we are not aware of any closed-form solution for this problem it is not possible to validate the accuracy of the proposed solution. In order to study the convergence of the solution we consider a straight crack that is placed along Ox axis and with the origin of the coordinate system placed at its center. The crack occupies the interval $[-1,1]$ and is subjected to uniform unit pore pressure. It is also assumed that the permeability coefficient of the medium is equal to 1. Fig. 7 displays the pore pressure p distribution along Ox axis for 4, 8, 12, 16, 20 and 24 integration points, respectively. Also, Fig. 8 presents the absolute relative error (the percentage of the absolute difference) between one calculation and its previous one with fewer integration points. It can be observed that the difference in the calculated

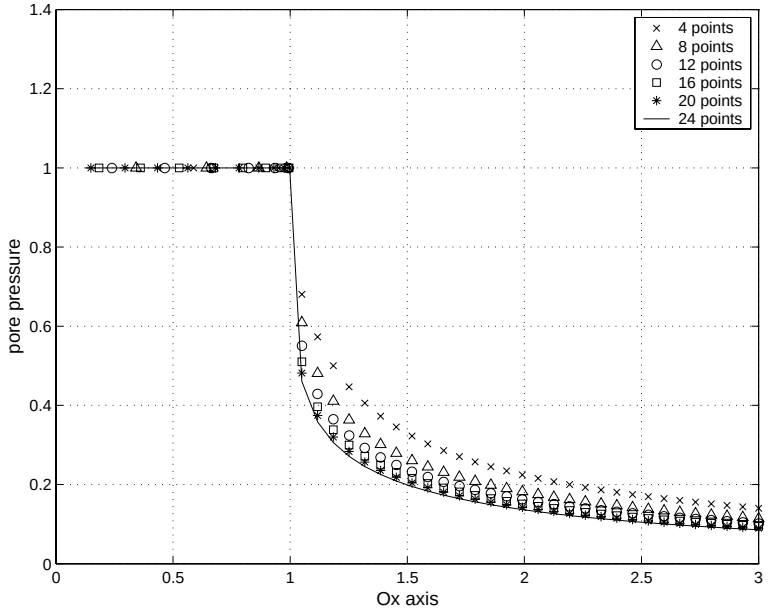

Fig. 7. Pore pressure distribution along Ox axis.

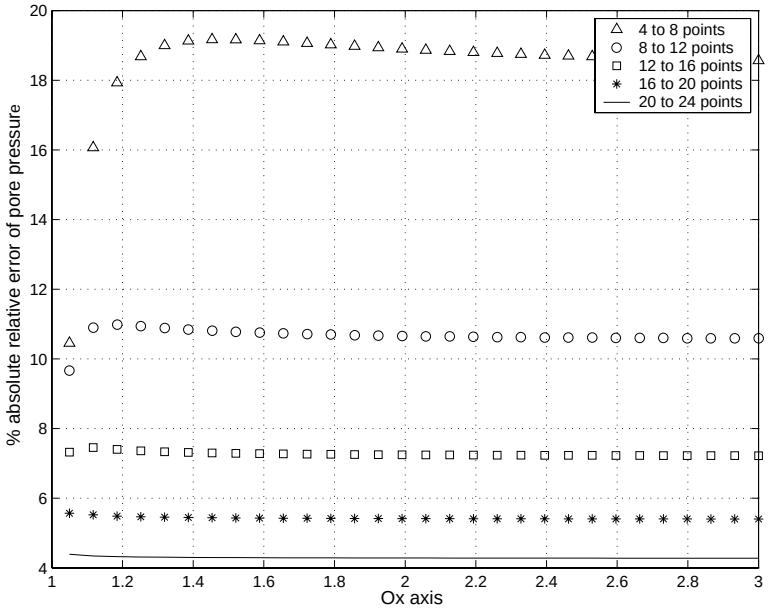

Fig. 8. Absolute relative error of the pore pressure calculation along Ox axis.

solution between 20 and 24 integration points is less than 5%, hence it is assumed that the solution converges above 20 integration points. Also, it should be preferred not to choose too many integrations points because the solution is sensitive to the round-off error. Figs. 9 and 10 display the fluid flow discharge along

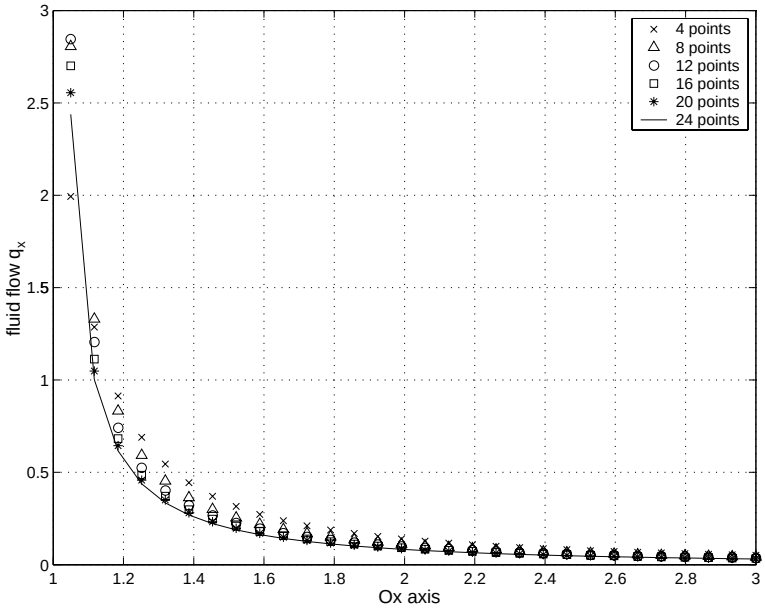

Fig. 9. Distribution of the component q_x of the fluid discharge vector along Ox axis.

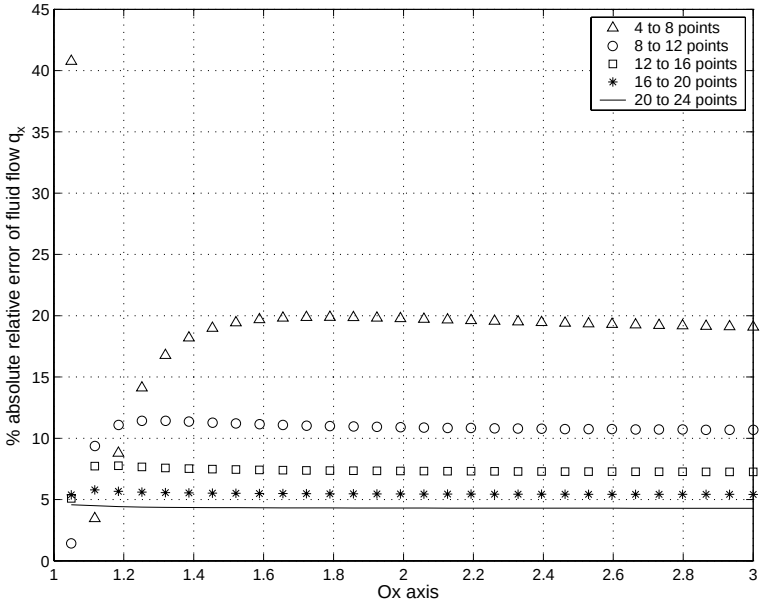

Fig. 10. Absolute relative error of the component q_x of the fluid discharge vector along Ox axis.

the Ox axis q_x and its relative error calculated as before. Moreover, Figs. 11–14 display the pore pressure p, the fluid flow q_y and their relative errors along Oy axis, respectively. The fluid flow q_y along Ox axis as well as q_x along Oy axis are not displayed since the result is practically equal to zero (values of order $O(10^{-14})$ as

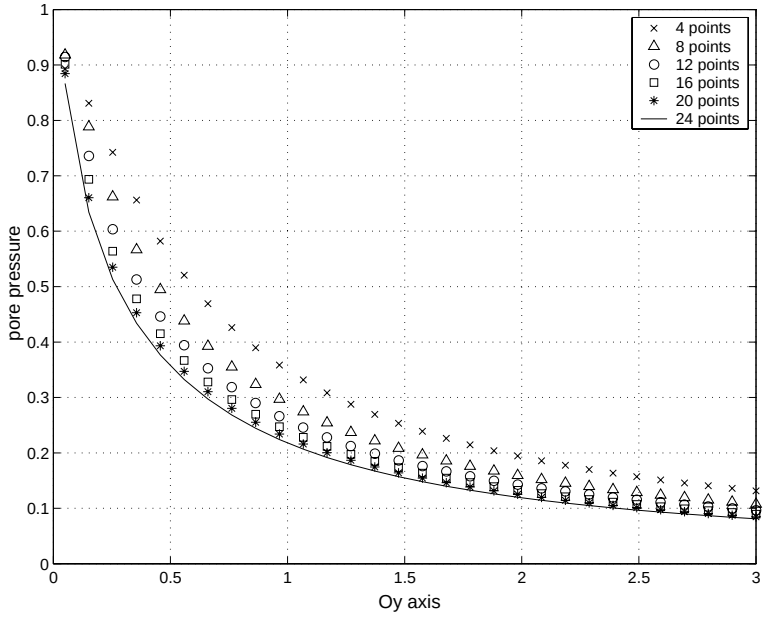

Fig. 11. Pore pressure distribution along *Oy* axis.

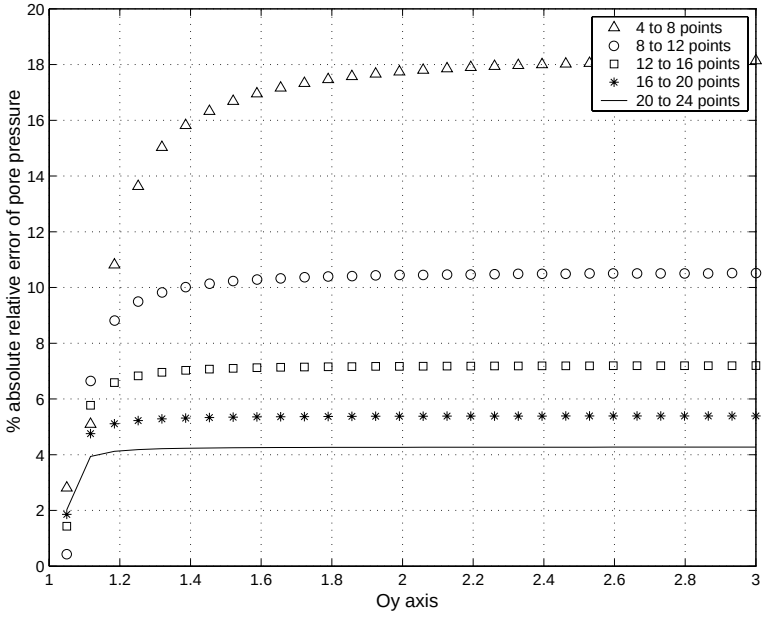

Fig. 12. Absolute relative error of the pore pressure calculation along *Oy* axis.

it was expected due to symmetry. Also, as it may be observed from (35), it is impossible to calculate the fluid flow q_y ($q_y = q_n$ in this case) on the crack. This is the reason for the high discrepancy of the fluid flow q_y

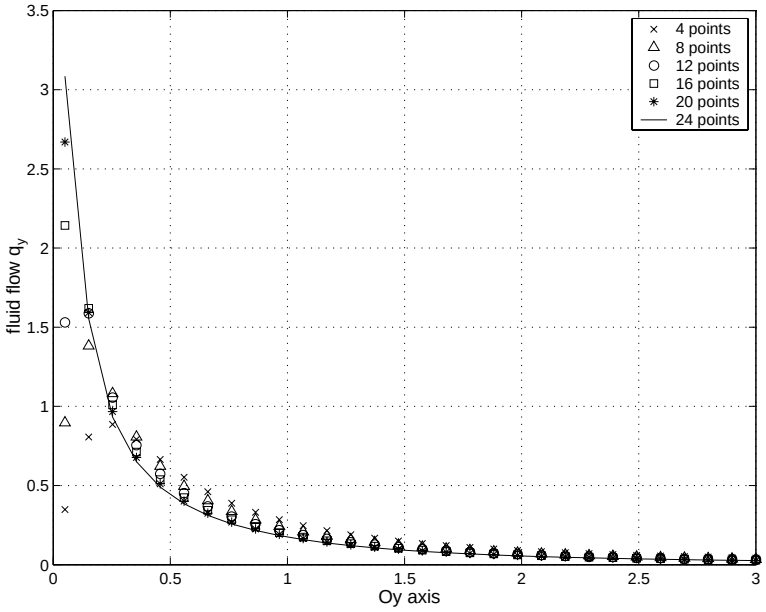

Fig. 13. Distribution of the component q_y of the fluid discharge vector along Oy axis.

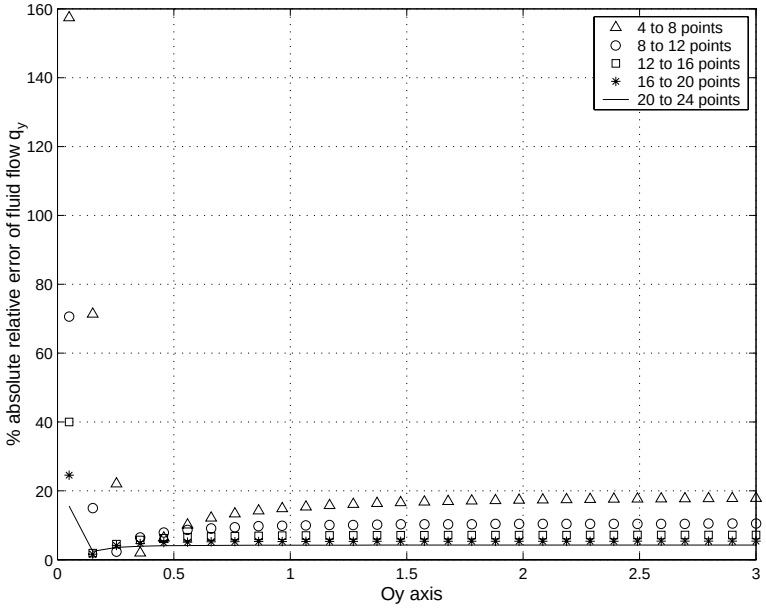

Fig. 14. Absolute relative error of the component q_y of the fluid discharge vector along Oy axis.

along Oy axis that is observed when the calculation point approaches zero (the origin of the coordinate system).

In order to illustrate the capabilities of the method we present two arbitrary examples of multiply fractured domains. In the first example we have considered three curvilinear cracks with Dirichlet boundary condition (i.e. fixed pore pressure distribution) applied on them. Figs. 15–17 display the pore pressure $p(z)$ and the fluid flow vector components along Ox ($q_x(z)$) and Oy ($q_y(z)$) directions, respectively. In this

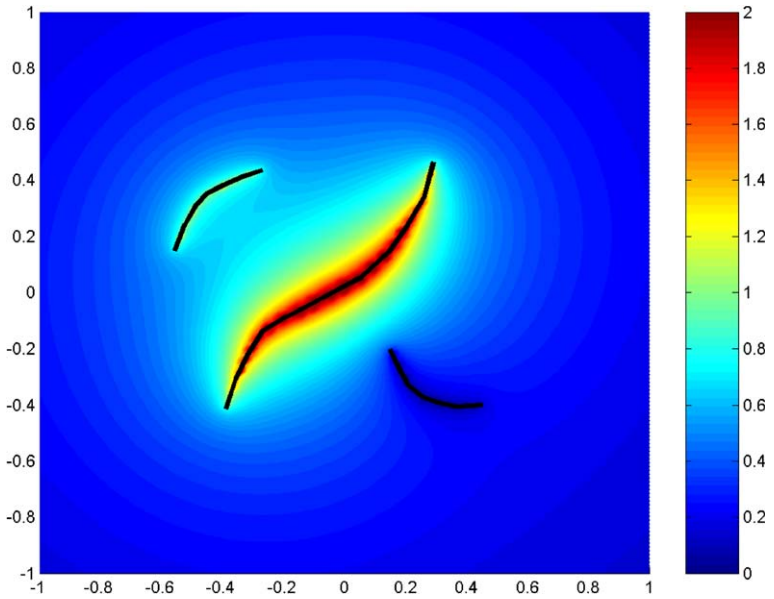

Fig. 15. Pore pressure distribution ($p(z)$) in the plane.

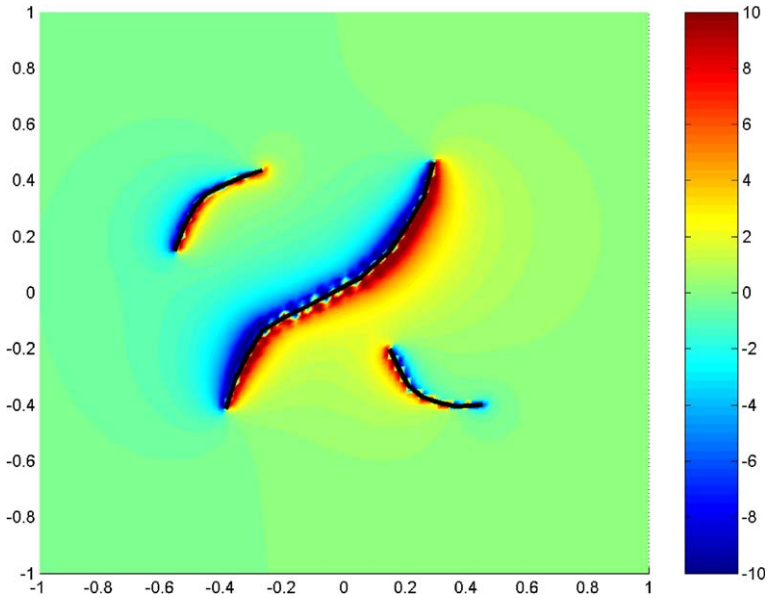

Fig. 16. Distribution of the fluid discharge component $q_x(z)$ in the plane.

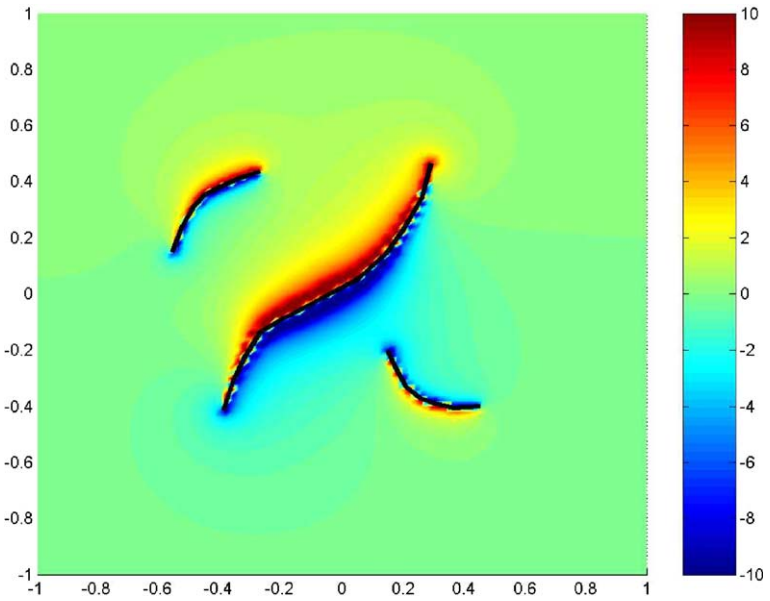

Fig. 17. Distribution of the fluid discharge component $q_y(z)$ in the plane.

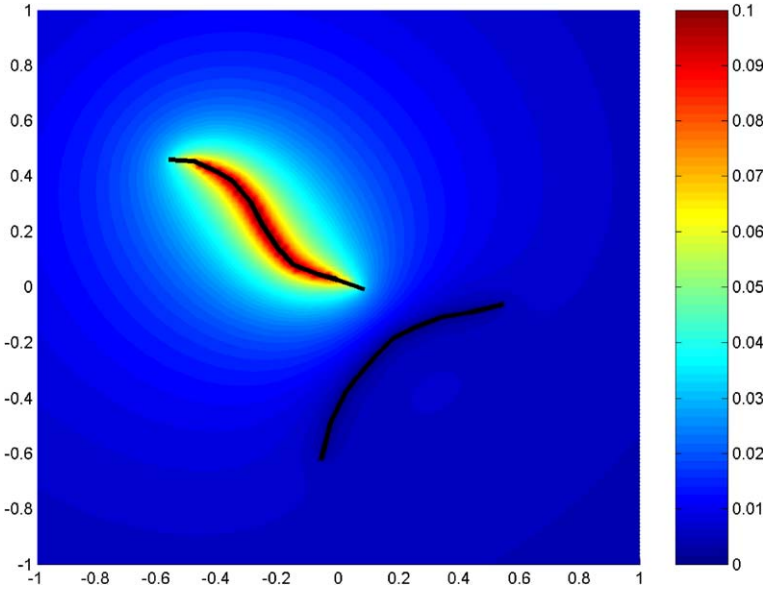

Fig. 18. Pore pressure distribution ($p(z)$) in the plane.

case, we have used 30 integration points per crack, a permeability coefficient $\lambda = 1$ and the following boundary conditions:

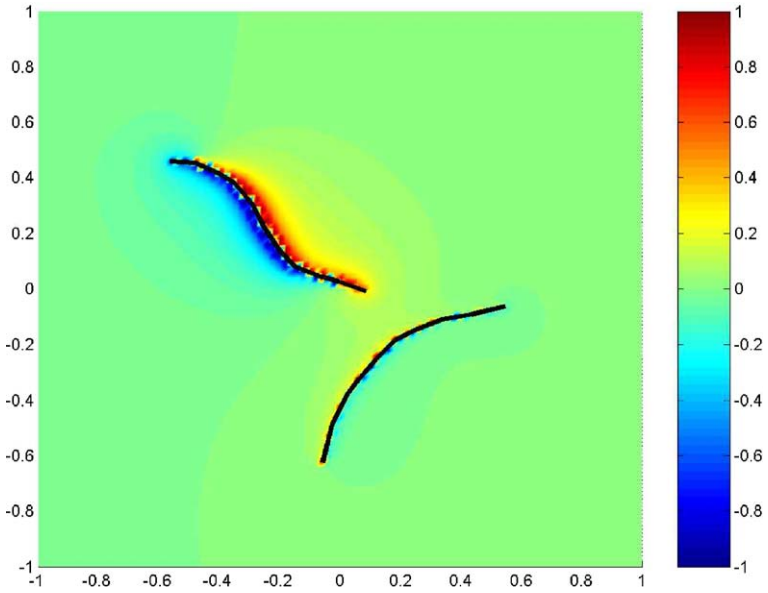

Fig. 19. Distribution of the fluid discharge component $q_x(z)$ in the plane.

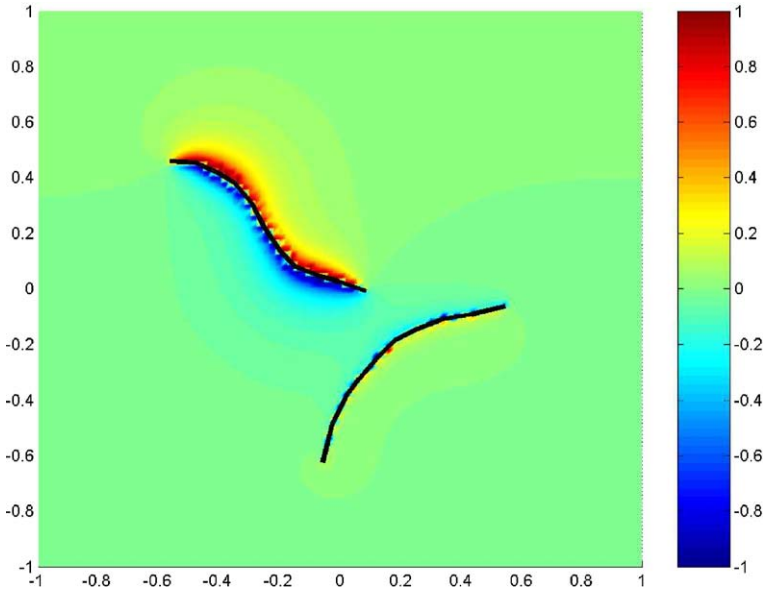

Fig. 20. Distribution of the fluid discharge component $q_y(z)$ in the plane.

(1) The crack located in the center is subjected under pressure given by $p(s) = 2 - \frac{4}{l^2}(s - l/2)^2$ (where s is a real variable that runs along the length of the crack and has as origin one of its tips and l is the length of the crack).
(2) The crack located in the upper left corner is under uniform pressure given by $p(s) = 1$.

(3) The other crack located in the lower right corner is subjected under constant pressure $p(s) = 0$ (cavitation).

On the second example, (Figs. 18–20) we consider two cracks in which the first one is under constant tangential fluid flow while there is a cavitation on the second one. Again, we have used $n = 30$, $\lambda = 1$ and the following boundary conditions:

(1) Tangential fluid flow $q_s(s) = \frac{8}{l^3}(s - l/2)^3$ is applied to the upper left crack. Note that this boundary condition satisfies the *Condition of Solubility* (Eq. (38)).
(2) The other crack located in the lower right corner is subjected to constant null pressure $p(s) = 0$ (cavitation).

Note that some instabilities that might arise near and/or on the cracks are due to the location of the points of the grid that we use. When a point is near an integration point, then its value tends to become singular. The only points very close to the integration points that the solution can be calculated are the collocation points. However, this phenomenon does not affect the behavior or the accuracy of the solution.

5. Concluding remarks

In a first step, the complete system of equations that depict the problem of steady-state flow in an isotropic porous medium containing an arbitrary system of cracks, thin strip inclusions, holes and point sources (or sinks) is presented. Next, a semi-analytical solution for steady-state fluid flow in multiply fractured isotropic media is, also, illustrated. The distribution of the pore pressure and the fluid flow on the fractured plane can be derived from either Dirichlet or Neumann boundary conditions specified along the crack surfaces. The numerical integration scheme of the derived solution converges rapidly to the solution and is easily implemented into a PC. Although the considered model is characterized by many simplifications (i.e. steady-state conditions, linearity, isotropy), it can find many useful applications in current engineering practice. For example, it may be used to test the accuracy of a numerical code (such as FEM, FDM or BEM), as a tool for quick back analysis of in situ fluid flow or pore pressure measurements, as a supplement to another numerical code for coupled thermo-hydro-mechanical problems etc.

The extension of the numerical algorithm in order to attack the problem of interaction between holes, cracks and thin strip inclusions is a straightforward task. Also, the generalization of the proposed theory to anisotropic porous media is a formidable task and will be presented in a future publication.

Acknowledgements

The financial support by the European Union Programmes "3F-Corinth (Faults, Fractures & Fluids)" under Contract No. ENK6-2000-0056 and McDUR Project entitled "Effects of the weathering on stone materials: Assessment of their mechanical durability" under Contract No. G6RD-CT-2000-00266 is kindly acknowledged here.

References

Banerjee, P.K., Butterfield, R., 1981. Boundary Element Methods in Engineering Science. McGraw-Hill, London.

Barenblatt, G.I., Zheltov, I.P., Kochina, I.N., 1960. Basic concepts in the theory of seepage of homogeneous liquids in fissured rocks. Prikl. Mat. Mekh. 24, 852–864.

Barzokas, D., Exadaktylos, G., 1995. Integral equations of thermoelasticity and thermoconductivity for cracked isotropic or anisotropic multiply connected bodies with reinforcement. Arch. Mech. 47 (2), 173–202.

Brebbia, C.A., Telles, J.C.F., Wrobel, L.C., 1984. Boundary Element Techniques. Springer, Berlin.

Brebbia, C.A., Dominguez, J., 1989. Boundary Elements, An Introductory Course, Computational Mechanics. McGraw-Hill, Southampton.

Erdogan, F., 1969. Approximate solutions of systems of singular integral equations. SIAM J. Appl. Math. 17(6), 1041–1059.

Erdogan, F., Gupta, G.D., 1972. On the numerical solution of singular integral equations. Quart. Appl. Math. 30, 525–534.

Evans, B., Wong, T.-F. (Eds.), 1992. Fault Mechanics and Transport Properties of Rocks. Academic Press Inc., San Diego.

Hartmann, F., 1989. Introduction to Boundary Elements. Springer, Berlin.

Hickman, S., Sibson, R., Bruhn, R., 1994. The mechanical involvement of fluids in faulting. US Geological Survey Menlopark, CA.

Hui, C.Y., Mukherjee, S., 1997. Evaluation of hypersingular integrals in the boundary element method by complex variable techniques. Int. J. Solids Struct. 34, 203–221.

Mikhlin, S.G., 1957. Integral Equations. Pergamon Press, London.

Muskhelishvili, N.I., 1953. Singular Integral Equations. P. Noordhoff Ltd., Groningen, Holland.

Parton, V.Z., Morozov, E.M., 1978. Elastic–Plastic Fracture Mechanics. Mir Publishers, Moscow.

Reddy, J.N., 1993. An Introduction to the Finite Element Method, second ed. McGraw-Hill, New York.

Sneddon, I.N., 1951. Fourier Transforms. McGraw-Hill, New York.

Warren, J.E., Root, P.J., 1963. The behavior of naturally fractured reservoirs. Soc. Pet. Eng. J. 3, 245–255.